

Undecidability of the fate of relaxation in one-dimensional quantum systems

Naoto Shiraishi* and Keiji Matsumoto†

2022/3/25

Abstract

We investigate the relaxation dynamics in an isolated quantum many-body system. The stationary value of an observable after relaxation is a topic of researches in the field of quantum thermalization, since thermalization is a relaxation phenomena where this stationary value coincides with the equilibrium value. Therefore, computing the stationary value in quantum many-body systems is regarded as an important problem. We, however, prove that the stationary value in quantum many-body systems is uncomputable. More precisely, we show that whether the stationary value is in the vicinity of a given value or not is an undecidable problem. Our undecidable result is still satisfied when we restrict our system to a one-dimensional shift-invariant system with nearest-neighbor interaction, our initial state to a product state of a state on a single site, and our observable to a shift-sum of a one-body observable. This result clearly shows that there is no general theorem or procedure to decide the presence or absence of thermalization in a given quantum many-body system.

Contents

1	Introduction	2
2	Background of thermalization and long-time average	3
3	Setup and main results	4
4	Proof of main theorems from Lemma 1	7
5	Strategy for the proof of Lemma 1	7
6	Proof of Lemma 1: (1) Classical Turing machine	8
6.1	Universal reversible Turing machine	8
6.2	Generalized URTM	10
6.3	The states, symbols, and tape of M_G	10
6.4	The move of M_G : the first step	11
6.5	The move of M_G : when $q \in Q$	12
6.6	The move of M_G : when $q \in Q_r$	12

*Department of physics, Gakushuin university, 1-5-1 Mejiro, Toshima-ku, Tokyo, 171-8588, Japan

†Quantum Computation Group, National Institute of Informatics, 2-1-2 Hitotsubashi, Chiyoda-ku, Tokyo 101-8430, Japan

7	Proof of Lemma 1: (2) Quantum partial isometry corresponding to M_G	12
7.1	Toy example of Feynman-Kitaev type Hamiltonian	12
7.2	Construction of quantum partial isometry for M_G	14
8	Proof of Lemma 1: (3) Evaluating \bar{A} for computational basis state	15
8.1	General expression of long-time average	15
8.2	Hamiltonian emulating M_G and effective Hamiltonian	16
8.3	Computing long-time average of A	16
9	Proof of Lemma 1: (4) Evaluating \bar{A} for superposition of computational basis states	18
9.1	Setting of the initial state and decoding of the input	18
9.2	Case when TM2 halts 1: decoding and expression of states	20
9.3	Case when TM2 halts 2: long-time average of A	21
9.4	Case when TM2 does not halt	23
10	Remarks	25
10.1	Dimension of the local Hilbert space	25
10.2	Exact value of \bar{A} in thermodynamic limit when TM2 halts	25
10.3	What happens if we numerically simulate this system?	26
10.4	Undecidability of thermalization	26
11	Concluding remarks	27

1 Introduction

Thermalization in quantum many-body systems have attracted interest of researchers in various research fields. In these fields, we investigate what determines the presence or absence of thermalization and how to understand thermalizing and non-thermalizing phenomena. This problem is an old longstanding problem that it has already been discussed by Boltzmann [1] and von Neumann [2]. Recent development of experimental techniques on cold atoms pushes this old problem toward a new step, and thermalization of isolated quantum many-body systems has been minutely examined in laboratory [3–7]. Elaborated experiments have revealed some unexpected behaviors including quantum many-body scars [8], which has recently been studied intensively [9–13]. In the theoretical approach, various suggestive notions including typicality of states [14–19] and dynamics [20–23], eigenstate thermalization hypothesis [24–29] and its violation [30–34], weak-version of eigenstate thermalization hypothesis [29, 35], the effective dimension [19, 36–39], the quantum many-body localization [40–46], generalized Gibbs ensemble [47–50] and many other important findings [51–54] have been raised and some aspects of thermalization have been well clarified (see a review paper [55]). However, the full understanding of thermalization is still far from our present position. Particularly, one of the central problem, determining whether a given system thermalizes or not, has still been left unsolved.

In this paper, we consider this problem by a completely different approach from conventional ones. We employ the viewpoint from theoretical computer science and quantum information, and prove that the above problem of thermalization is undecidable. More precisely, we prove that the expectation value of an observable A after relaxation with a given

Hamiltonian H of a one-dimensional system is undecidable. Our result of undecidability is still valid if we restrict the class of the observable A as a shift sum of a given one-body observable, the Hamiltonian H as a shift-invariant nearest-neighbor interaction, and the initial state as a product state of identical states on a single site (except the first site). This result directly implies that there is no general procedure to decide the presence or absence of thermalization, obviously no general theorem.

Undecidability sometimes appears in physics. Examples are dynamical systems [56], repeated quantum measurement [57], and spectral gap in quantum many-body systems [58], and our finding tells that quantum thermalization stands in this line. Our proof is inspired by the following two tools: the reduction to the halting problem of Turing machine [59, 60] and Feynman-Kitaev type quantum emulation of classical machines [61, 62]. With several technical ideas, we successfully construct a quantum many-body systems where the destination after relaxation is determined by the halting problem of Turing machine.

This paper is organized as follows: In Sec. 2, we provide a pedagogical review of the motivation and the problem of quantum thermalization. In Sec. 3, we state two main theorems and a technical lemma. The latter lemma is the most important result in the theoretical aspect. In Sec. 4, we derive two main theorems from the technical lemma. The remainder of this paper is devoted to prove this lemma. In Sec. 5, we briefly sketch the proof strategy. In Sec. 6, we introduce a classical universal reversible Turing machine, which is responsible for the halting problem. In Sec. 7, we construct the Hamiltonian of the quantum system emulating the classical dynamics of the Turing machine. Since the details of dynamics of our quantum system is a little complicated, in Sec. 8 we introduce an analogous setting to our original one but easier to treat, and solve this dynamics. In Sec. 9, we go back to the original setting and construct the initial state with which the expectation value after relaxation is indeed undecidable.

2 Background of thermalization and long-time average

Before going to our main result, we summarize the problem of thermalization for readers who are not familiar with this topic. If a reader is familiar with it, one can skip this section.

In the research field of quantum thermalization, we mainly consider whether a quantum many-body system with a Hamiltonian H at the initial state $|\psi\rangle$ thermalizes (with respect to an observable A) or not. A state $|\phi\rangle$ is called *thermal* with respect to an observable A if its expectation value of A is close to its equilibrium value:

$$\langle\phi|A|\phi\rangle \simeq \text{Tr}[A\rho_{\text{MC}}], \quad (1)$$

where ρ_{MC} is a microcanonical state with energy $\langle\phi|H|\phi\rangle$. The symbol \simeq means that both-hand sides coincide in the thermodynamic limit¹. We call that an initial state $|\psi\rangle$ under the Hamiltonian H *thermalizes* with respect to A if $|\psi(t)\rangle := e^{-iHt}|\psi\rangle$ is thermal with respect to A for almost all t :

$$\lim_{T \rightarrow \infty} \frac{1}{T} \int_0^T dt \chi(\langle\psi(t)|A|\psi(t)\rangle \simeq \text{Tr}[A\rho_{\text{MC}}]) \simeq 1, \quad (2)$$

¹If $A = O(1)$, $A \sim B$ means $\lim_{V \rightarrow \infty} (A - B) = 0$. If $A = O(V)$, $A \sim B$ means $\lim_{V \rightarrow \infty} \left(\frac{A}{V} - \frac{B}{V} \right) = 0$.

where $\chi(\cdot)$ is a characteristic function which takes 1 (resp. 0) if the statement inside the bracket is true (resp. false). Note that due to the quantum recurrence theorem [63], for any T' there exists $\tau > T'$ such that the state at time τ , $|\psi(\tau)\rangle$, and the initial state $|\psi(0)\rangle$ is arbitrarily close. Our definition of thermalization allows recurrence while recurrence time should become extremely long in a large system.

Let $\bar{A} := \lim_{T \rightarrow \infty} \frac{1}{T} \int_0^T dt \langle \psi(t) | A | \psi(t) \rangle$ be the long-time average of A . Then, an initial state thermalizes if the following two conditions are satisfied:

- (Relaxation): The time-series fluctuation around the long-time average \bar{A} converges to zero:

$$\lim_{T \rightarrow \infty} \frac{1}{T} \int_0^T dt (\langle \psi(t) | A | \psi(t) \rangle - \bar{A})^2 \simeq 0. \quad (3)$$

- (Convergence to the equilibrium value): The long-time average \bar{A} converges to the equilibrium value $\text{Tr}[A\rho_{\text{MC}}]$:

$$\bar{A} \simeq \text{Tr}[A\rho_{\text{MC}}]. \quad (4)$$

The former condition, relaxation, is proven for initial states under some condition (a diverging effective dimension) [36–38] and this condition is shown to be fulfilled analytically in physically plausible initial states [39]. Thus, the remaining hard task is to handle the latter condition, convergence to the equilibrium value. This is why various concepts and arguments raised in the field of quantum thermalization concern the long-time average and the equilibrium value.

The main goal of this paper is to prove the incomputability of the value of the long-time average \bar{A} . In other words, we have no general procedure to detect the behavior of quantum many-body systems after relaxation.

3 Setup and main results

Consider a one-dimensional chain of d -level quantum systems with the periodic boundary condition, whose underlying local Hilbert space is denoted by \mathcal{H} .

Suppose that the Hamiltonian of this chain H is shift invariant and contains only 1-body terms and nearest-neighbor 2-body interactions. We set the length of the system as L . Let A be a non-negative observable of \mathcal{H} , and A_L denote the normalized spatial average of A 's:

$$A_L := \frac{1}{L} \sum_{i=1}^L A_i, \quad (5)$$

where A_i is the operator A acting on the site i . Without confusion, we crudely use the symbol A also for representing its spatial average A_L with general system size. Our interest is a long-time average of A_L :

$$\bar{A}(H, \rho) := \lim_{L \rightarrow \infty} \lim_{T \rightarrow \infty} \frac{1}{LT} \int_0^T \text{Tr}[e^{-iHt} \rho_L e^{iHt} A_L] dt, \quad (6)$$

where ρ_L is the initial state of the system with length L^2 . Whenever without confusing, dependency of \bar{A} on H and ρ is dropped.

²More precisely, we first introduce a state ρ with infinite length, and define ρ_L as the restriction of the state ρ to the first L consecutive sites.

We argue, roughly, that \overline{A} is incomputable³. To state our claim in a rigorous manner, we define two decision problems with a promise; STA (state time average) and HTA (Hamiltonian time average).

[STA]: The dimension of the local Hilbert space $d = \dim \mathcal{H}$, a Hamiltonian H , and an observable A are fixed, and H and A are computable.

Input: a density operator ρ .

Promise: Either $\overline{A} \in [c + \varepsilon_1, c - \varepsilon_1]$ or $\overline{A} \notin [c + \varepsilon_2, c - \varepsilon_2]$ with $0 < \varepsilon_1 < \varepsilon_2$ holds.

Decision problem: Decide which of the above two holds.

[HTA]: The dimension of the local Hilbert space $d = \dim \mathcal{H}$, an observable A , and an initial state ρ are fixed, and A and ρ are computable.

Input: a Hamiltonian H .

Promise: Either $\overline{A} \in [c + \varepsilon_1, c - \varepsilon_1]$ or $\overline{A} \notin [c + \varepsilon_2, c - \varepsilon_2]$ with $0 < \varepsilon_1 < \varepsilon_2$ holds.

Decision problem: Decide which of the above two holds.

We now state our main theorems, which claim that these decision problems are undecidable. Below, d_0 is a fixed finite but sufficiently large number, whose rough estimation is presented in Sec. 10.1.

Theorem 1

Suppose $d \geq d_0$. Then, there exists a shift-invariant Hamiltonian H with 1-body terms and 2-body nearest-neighbor interaction terms having the following properties:

Let A be an arbitrary observable on a single site. Then, for any $\varepsilon_2 > 0$, there exists an operator A' with $\|A - A'\| \leq \varepsilon_2$ such that the STA for A' with any $\varepsilon_1 \leq \frac{1}{5}\varepsilon_2$ is undecidable. This remains valid even if the initial state ρ is restricted to a product state of a pure state of a single site in the form of

$$\rho_L = |\phi_0\rangle |\phi_1\rangle^{\otimes L-1}. \quad (7)$$

³To make such an assertion appropriately, some vocabulary from computer science are necessary: We say the operator A is computable if any component (with respect to some standard basis) of A can be computed by a Turing machine with any specified accuracy (So the inputs of a Turing machine are the indices of the components and the integer specifying the accuracy). Also, the Hamiltonian and the density operator over the one-dimensional chain is computable if its restriction to the finite system size (L) is computable. In our case, the Hamiltonian is computable if and only if its 1- and 2- body terms are computable.

Whenever we say an operator A is an input to the problem, we mean that the bit string describing A is given to a Turing machine as the input. Here, the map of the bit string to an arbitrary component should be computable up to any given accuracy. When the input is an observable or a state over $\mathcal{H}^{\otimes \infty}$, again the bit string description is given. The computability of the map of the bit string to the observable or the state is defined considering restriction to the finite-size system.

Theorem 2

Suppose $d \geq d_0$. Then, there exists a pure state ρ in the form of Eq. (7) having the following properties:

Let A be an arbitrary observable on a single site that is not a constant multiple of the identity. Then, for some ε_2 and ε_1 , the HTA is undecidable. This remains valid even if the Hamiltonian H is restricted to a shift-invariant Hamiltonian H with 1-body terms and 2-body nearest-neighbor interaction terms.

These two theorems are in fact different rewritings of the following technical lemma. This lemma claims that there exists a shift-invariant one-dimensional Hamiltonian which decodes the input code from Hamiltonian itself and emulates the dynamics of a universal reversible Turing machine (URTM) properly.

Lemma 1

Suppose that the dimension of the local Hilbert space $d \geq d_0$ is fixed. A complete orthonormal system (CONS) of the local Hilbert space $\{|e_i\rangle\}_{i=0}^{d-1}$ and an observable A over \mathcal{H} with $\langle e_1|A|e_1\rangle = 0$ and $\langle e_2|A|e_2\rangle > 0$ are given arbitrarily. Then, for any $\eta > 0$ there exist a shift-invariant Hamiltonian H (which depends on the CONS) and a set of computable unitary operators over \mathcal{H} denoted by $\mathcal{V}_{A,\eta}$ (which depends also on A and $\eta > 0$) with the following properties:

- H consists of 1-body terms and 2-body nearest-neighbor interaction terms.
- For any $V \in \mathcal{V}_{A,\eta}$, $V|e_0\rangle = |e_0\rangle$ is satisfied.
- $\mathcal{V}_{A,\eta}$ is large enough to encode all the bit strings into $V \in \mathcal{V}_{A,\eta}$.
- By setting the initial state as

$$|\psi_{V,L}\rangle := V|e_0\rangle \otimes (V|e_1\rangle)^{\otimes L-1}, \quad (8)$$

then

$$\min\{\overline{A}(H, \psi_V), \overline{VAV^\dagger}(H, \psi_V)\} \geq \left(\frac{1}{4} - \eta\right) \langle e_2|A|e_2\rangle \quad (9)$$

is satisfied if and only if the URTM halts on the input binary string corresponding to V , and

$$\max\{\overline{A}(H, \psi_V), \overline{VAV^\dagger}(H, \psi_V)\} \leq \eta \quad (10)$$

is satisfied if and only if the URTM does not halt on the input binary string corresponding to V .

Here, we bound both \overline{A} and $\overline{VAV^\dagger}$ in order to treat STA and HTA simultaneously. By this lemma, we can prove that the halting problem, a well-known undecidable problem, is not easier than STA nor HTA: So the latters are also undecidable.

4 Proof of main theorems from Lemma 1

Below, without loss of generality, we suppose $\langle e_1|A|e_1\rangle = 0$. This condition can be met by subtracting a constant factor. We also set the target value c in STA and HTA to zero.

Proof of Theorem 1. We argue that the STA for the following state family

$$\bigcup_{A:\langle e_1|A|e_1\rangle=0} \{|\psi_V\rangle \mid |\psi_{V,L}\rangle = V|e_0\rangle \otimes (V|e_1\rangle)^{\otimes L-1}, V \in \mathcal{V}_{A',\eta}\} \quad (11)$$

is undecidable, where the operator A' is properly chosen as

$$A' = \begin{cases} \varepsilon_2 |e_2\rangle \langle e_2| + A & \text{if } \langle e_2|A|e_2\rangle \geq 0, \\ -\varepsilon_2 |e_2\rangle \langle e_2| - A & \text{if } \langle e_2|A|e_2\rangle < 0. \end{cases} \quad (12)$$

We also set $\eta = \varepsilon_1 \leq \frac{1}{5}\varepsilon_2$. Then, for sufficiently small $\eta = \varepsilon_1$

$$\eta = \varepsilon_1 \leq \frac{1}{5}\varepsilon_2 \leq \frac{1}{5} |\langle e_2|A'|e_2\rangle| < \left(\frac{1}{4} - \eta\right) |\langle e_2|A'|e_2\rangle| \quad (13)$$

is satisfied, and Lemma 1 suggests that the STA with these parameters is undecidable. \square

Proof of Theorem 2. We fix two given states $|e_0\rangle$ and $|e_1\rangle$, and choose $|e_2\rangle$ such that $\langle e_2|A|e_2\rangle \neq 0$. Without loss of generality, we suppose $\langle e_1|A|e_1\rangle > 0$. (In case of $\langle e_1|A|e_1\rangle < 0$, we obtain an analogous conclusion by setting $A \rightarrow -A$.) Consider an A -dependent family of Hamiltonians given as

$$\{H_V \mid H_{V,L} = (V^\dagger)^{\otimes L} H_L V^{\otimes L}, V \in \mathcal{V}_{A,\eta}\}. \quad (14)$$

Recall that H_L given in Lemma 1 depends on the choice of the CONS. Meantime, as $|e_0\rangle$ and $|e_1\rangle$ are chosen independent of A , $|\psi_{I,L}\rangle = |e_0\rangle \otimes |e_1\rangle^{\otimes L-1}$ is also independent of A .

Since $\overline{A}(H_V, \psi_I) = \overline{VAV^\dagger}(H, \psi_V)$, Lemma 1 implies that either

$$\overline{A}(H_V, \psi_I) = \overline{VAV^\dagger}(H, \psi_V) \geq \left(\frac{1}{4} - \eta\right) \langle e_2|A'|e_2\rangle \quad (15)$$

or

$$\overline{A}(H_V, \psi_I) = \overline{VAV^\dagger}(H, \psi_V) \leq \varepsilon \quad (16)$$

holds. Thus, these two alternatives define an HTA.

Observe that the former alternative implies the negation of (10) (non-halting case), and the latter alternative implies the negation of (9) (halting case). Hence, this HTA is not easier than the decision problem posed in Lemma 1, so is not easier than the halting problem. \square

5 Strategy for the proof of Lemma 1

The rest of this paper is devoted to prove Lemma 1. Before going to the details of the proof, we here sketch the strategy of the proof.

We first introduce a classical reversible Turing machine which is emulated by our quantum system (Sec. 6). The classical reversible Turing machine has two types of cells: M-cells, and

A-cells (see Fig. 1). The decode of an input code and simulation of a URTM is performed in M-cells, while A-cells are responsible for the change of \bar{A} (the long-time average of A) in case of halting. Namely, we emulate the URTM in M-cells, and if and only if the URTM halts, then we start flipping the state of A-cells. For the reason discussed later, we set vast majority of cells to A-cells, and small fraction of cells to M-cells.

We construct a quantum system which emulates the above classical reversible Turing machine (Secs.7-9). The Hamiltonian is constructed as in a similar manner to the Feynman-Kitaev Hamiltonian without a clock, where one-step time evolution of the classical Turing machine corresponds to an application of a quantum partial isometry as a quantum walk (Sec. 7). The idea of the Feynman-Kitaev Hamiltonian is first demonstrated with a simple toy example (Sec. 7.1), and then we construct the quantum isometry for our classical Turing machine (Sec. 7.2).

Since the dynamics of our system is a little complicated, we first introduce an analogous setting to our original one but easier to analyze, where the initial state is a non-shift-invariant computational basis state representing the input code (Sec. 8). In this analogous setting, we demonstrate how \bar{A} varies depending on the halting/non-halting of the URTM. In this case, the dynamics is fully solvable since the effective Hamiltonian for this initial state can be expressed as a tridiagonal matrix, which can be exactly diagonalized.

We then proceed to the our original setting, a shift-invariant initial state (except the site 1), where the initial state is a superposition of computational basis states (Sec. 9). In this case, we elongate the dimension of the local Hilbert space in order to decode the input code for the URTM from shift-invariant 2 q-bit sequences before the URTM runs. The first two subsections (Sec. 9.1 and Sec. 9.2) are devoted to describe the decoding of the input code from a uniform initial state. Resorting the law of large numbers, we demonstrate that the input code is successfully decoded with arbitrarily high probability amplitude by choosing proper parameters. In the subsequent two subsections, we describe how \bar{A} varies in case of halting and non-halting. If the URTM halts, it starts flipping spins in A-cells to increase the value of A . The stable state of the corresponding quantum walk is uniformly distributed over all the states traversed by this discrete time dynamics, so the expectation of A becomes large if the URTM halts (Sec. 9.3). On the other hand, since the URTM is simulated on relatively small numbers of sites (M-cells), which are sparsely located in the 1D-chain, if the URTM does not halt, an overwhelming part of the system (A-cells) remains unchanged (Sec. 9.4).

6 Proof of Lemma 1: (1) Classical Turing machine

6.1 Universal reversible Turing machine

Let TM2 be a URTM characterized by the set $(Q, \Gamma, q_0, q_f, s_0, \delta)$. Here, Q is the set of states of the finite control, Γ is the set of tape alphabet symbols, q_0 and q_f are the initial and the final state of the finite control respectively, s_0 is the blank symbol, and δ is the transition function. The set Γ contains the symbol \square , which stands for the left-most cell. Without loss of generality, we suppose the followings:

1. We essentially use the quadruple form, that is, split each step into the two sub-steps: The first sub-step is rewriting of the state and the symbol, and the second sub-step is the move of the tape head. To realize such moves of the machine, we set $Q := Q_m \times Q_u$

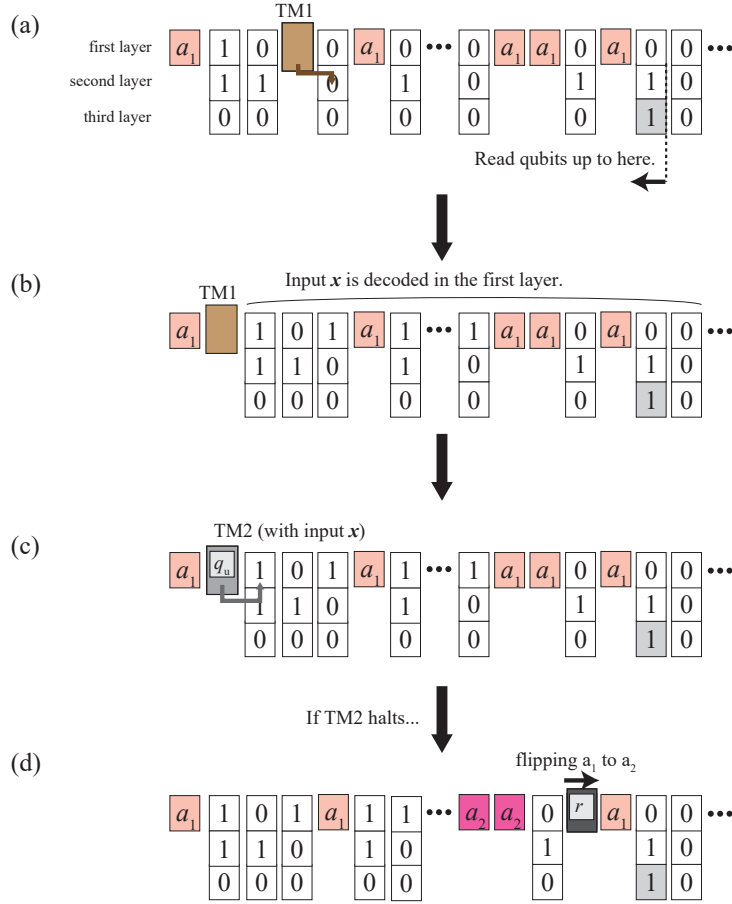


Figure 1: Schematic of the dynamics and the structure of the emulated classical machine. Two types of cells, M-cell and A-cell, and a finite control sit in a single line. The M-cells are three-layered colored in white, and the A-cells are colored in red. (a) TM1 decodes the input code x for TM2 from the second and third layers of M-cells. The relative frequency of 1's in the second layer in binary expansion is set to x , and the leftmost 1 in the third layer (colored in gray) tells how long TM1 reads cells in the second layer and how many digits it decodes. Note that TM1 and TM2 pass through A-cells. (b) After decoding of TM1, the input code x is written in the first layer of M-cells. (c) When TM1 stops, then a universal reversible Turing machine TM2 starts moving. If TM2 does not halt, TM2 eventually passes the periodic boundary and then TM2 stops its move. (d) If TM2 halts, then TM3 start flipping the state in A-cells from a_1 to a_2 , which changes the value of A .

with $Q_m := \{m_0, m_1\}$, where $q_m \in Q_m$ is used to represent the two distinct sub-steps. It equals m_0 when rewriting and m_1 when moving the tape head. At every step, the value of q_m is flipped, so that the rewriting (other than the Q_m part) and the move of the tape occurs alternately. This is for the sake of clarity and at the same time to realize the move of the tape head to the left by a two-body interaction.

2. We suppose that TM2 has *unique direction property*: Q_u is split into three disjoint subsets, Q_+ , Q_- and Q_0 (i.e., $Q_u = Q_+ \cup Q_- \cup Q_0$). The state q_u is in Q_+ (resp. Q_-) if and only if the tape head has moved to the right (resp. left), and in Q_0 if and only if the tape head has not moved. We promise that $q_0 \in Q_m \otimes Q_+$ and $q_f \in Q_m \otimes Q_-$.

3. The tape head of the initial configuration is at the left most cell, and the Q_m part equals m_1 . Hence, at the first step it moves to the right.

6.2 Generalized URTM

A generalized URTM, with a single tape with finite length, is almost the same as the above URTM, except for the following respects:

- The finite control sits between the two cells of the tape, and can read only one of the two adjacent cells in a single step. If it reads the cell right (left) to it, it moves to the right (left) or does not move. Each element q of the extended state space Q (we employ the same symbol for this extended space for brevity) tells which cell will interact with the finite control in this step.
- (Unique pairing property) For the sake of reversibility, we assume the following: Each element q of the state space Q tells the previous position of the finite control, and the cell it has interacted with. In analogy with the unique direction property of an RTM [64], we call this property as a unique pairing property.
- There are several configuration with no successor. For example, no successor is defined if the machine runs out of the space.

Any RTM can be simulated by a generalized RTM, as long as the length of the tape suffices.

6.3 The states, symbols, and tape of M_G

We define the set of states and symbols of M_G as

$$Q \cup Q_r = (Q_m \times Q_u) \cup Q_r, \quad (17)$$

$$\bar{\Gamma} \times \Gamma_A = (\Gamma \cup \{s_1\}) \times \Gamma_A, \quad (18)$$

where we set

$$Q_m := \{m_0, m_1\}, \quad (19)$$

$$Q_r := \{r\}, \quad (20)$$

$$\bar{\Gamma} := \Gamma \cup \{s_1\}, \quad (21)$$

$$\Gamma_A := \{a_1, a_2\}. \quad (22)$$

Here, $Q_m \times Q_u$ represents the states of the finite control of the URTM called TM2, and $Q_r = \{r\}$ is the sign for TM3, which flips the states in A-cells (Another Turing machine called TM1 is introduced later). The alphabets Γ and Γ_A appear in two distinct types of cells called *M-cells* and *A-cells* respectively. The symbol s_1 is a sign that this cell is an A-cell. Note that Γ contains the blank symbol s_0 . We compile these symbols in Fig. 2.

Out of the $L - 1$ cells, $\lfloor \alpha(L - 1) \rfloor$ cells are filled with symbols from $\Gamma \times \Gamma_A$, which serve as M-cells, and $\lceil (1 - \alpha)(L - 1) \rceil$ cells are filled with $\{s_1\} \times \Gamma_A$, which serve as A-cells. M-cells simulate TM2, and A-cells inflate the value of the observable A in case of halting. The rate α will be taken sufficiently small to observe the gap between the halting case and the

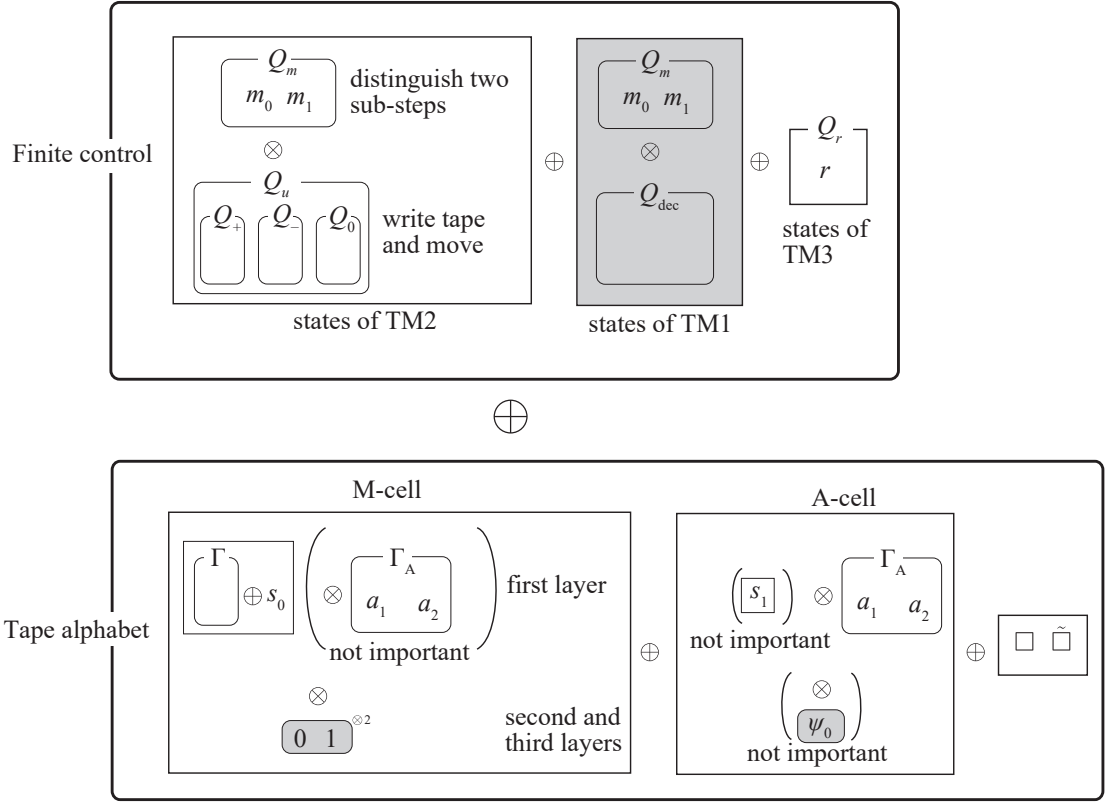


Figure 2: Summary of possible states of a single site in the quantum system. The symbols in gray areas are for decoding of the input of TM2, which will be introduced in Sec. 9.1.

non-halting case (i.e., almost all cells are set as A-cells, though the number of M-cells is also sufficiently large in $L \rightarrow \infty$ limit).

Initially, M_G 's state is set to (m_0, q_0) , and the input of TM2 is written on the M-cells in the right of the finite control. The Γ_A -part of the cell is set to a_1 . Cells in the left of the finite control is set to the blank cell s_0 . Below, for brevity we leave off the symbols $\lfloor \cdot \rfloor$ and $\lceil \cdot \rceil$ and also drop -1 , as L is large enough (i.e., we write αL and $(1 - \alpha)L$ instead of $\lfloor \alpha(L - 1) \rfloor$ and $\lceil (1 - \alpha)(L - 1) \rceil$).

6.4 The move of M_G : the first step

When M_G is in the initial state (m_0, q_0) , this RTM not only mimic the move of TM2 but also prepare the cell with \square . The finite control reads the site on the right of it, and rewrite its Γ -part as $s_0 \rightarrow \square$ and $s_1 \rightarrow \square'$ (There are no other possibility in legal configurations). We employ two different symbols \square and \square' only for satisfying the reversibility, and \square and \square' plays completely the same role: telling the left/right end of the tape. Therefore, in the remainder of this paper, we do not distinguish \square' from \square .

At the first step, the state and the position of the finite control will be changed in the same manner as the TM2's first step. Hence, first it evolves to (m_1, q) , and then it moves to the right and evolves to (m_0, q) .

6.5 The move of M_G : when $q \in Q$

While the state of the finite control q is in Q , M_G simulates TM2 in M-cells, and it virtually ignores A-cells (see Fig. 1.(c)). The finite control basically reads the cell at its right, except for the case that the position is changed to the left.

- If $q_m = m_0$, it reads the cell in its right. If it is an M-cell, the machine updates its state of Q_u part, q_u say, and the symbol in the cell according to the transition function δ . At the same time, Q_m part of the finite control, q_m say, evolves to m_1 . If it is an A-cell, q_u does not change and q_m simply evolves to m_1 .
- If $q_m = m_1$ and $q_u \in Q_+$, the finite control is swapped with the cell in its right, and q_m evolves to m_0 .
- If $q_m = m_1$ and $q_u \in Q_-$, the finite control is swapped with the cell in its left, and q_m evolves to m_0 .
- If $q_m = m_1$ and $q_u \in Q_0$, the finite control does not move, and q_m simply evolves to m_0 .

If $q_m = m_1$, the previous partner of the finite control is the cell on the right of it, and its previous position is the same as the present position. If $q_m = m_0$ and $q_u \in Q_+$ (resp. $q_u \in Q_-$), the previous partner of the finite control is the cell on the left (resp. right) of it, and previous position is at the left (resp. right) of the previous partner.

Eventually, the machine may run out of the tape: In case of the periodic boundary condition, the finite control reads the symbol \square with $q_u \in Q_+ \setminus \{q_0\}$. Since these states are illegal configurations, no successor is defined to them.

If the machine runs into the halting state q_f , then the finite control evolves into the state $r \in Q_r$. The dynamics after halting is given in the next subsection.

6.6 The move of M_G : when $q \in Q_r$

If the machine halts and the state of the finite control is in $r \in Q_r$, then TM3 starts flipping the state in A-cells from a_1 to a_2 (Fig. 1.(d)). If the cell on the right of the finite control is an A-cell with its state a_1 , then the head flips the state to a_2 and moves right. If the cell on the right of the finite control is an M-cell, then the finite control just moves right. If the cell on the right of the finite control is an A-cell with its state a_2 , which implies that all of the A-cells have already been flipped to a_2 and the finite control have gone around the periodic system, then TM3 stops.

7 Proof of Lemma 1: (2) Quantum partial isometry corresponding to M_G

7.1 Toy example of Feynman-Kitaev type Hamiltonian

Before constructing the quantum partial isometry for M_G , for readers who are not familiar with emulation of classical machines by quantum systems, we here demonstrate a toy example of a quantum partial isometry emulating a very simple classical machine. If a reader

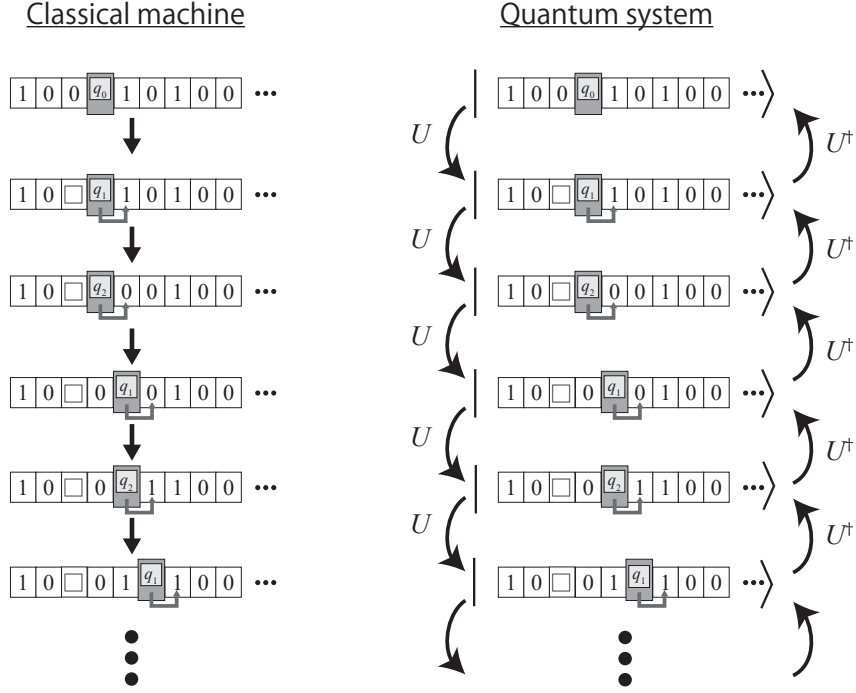


Figure 3: The dynamics of the toy example of a classical machine introduced in Sec. 7.1, and the corresponding quantum partial isometry U .

is familiar with this topic, one can skip this subsection and start reading the subsection entitled “Construction of quantum partial isometry for M_G ”.

We consider a simple classical machine, flipping bits with moving from left to right on a single line of cells. The finite control also settles in this line. The finite control takes three possible states, q_0 , q_1 and q_2 , and the transition rule of this machine is the following (see also Fig. 3):

1. If the state of the finite control is q_0 , then the state of the finite control evolves to q_1 . At the same time, the cell on the left of the finite control is flipped to \square (if the cell is 1) or $\tilde{\square}$ (if the cell is 0).
2. If the state of the finite control is q_1 and the cell on the right of the finite control is neither \square nor $\tilde{\square}$, then the machine flips the bit (i.e., $0 \rightarrow 1$ and $1 \rightarrow 0$) in the cell on the right of the finite control. At the same time, the state of the finite control evolves to q_2 .
3. If the state of the finite control is q_2 , then the finite control moves to right. At the same time, the state of the finite control evolves to q_1 .
4. If the state of the finite control is q_1 and the cell on the right of the finite control is \square or $\tilde{\square}$, then the machine stops.

We emulate the above classical machine by a one-dimensional quantum system with nearest-neighbor interaction. The local Hilbert space is spanned by seven states

$$\{|0\rangle, |1\rangle, |q_0\rangle, |q_1\rangle, |q_2\rangle, |\square\rangle, |\tilde{\square}\rangle\}.$$

The local quantum isometry on the sites i and $i + 1$ is given as

$$U_{i,i+1} = U_{i,i+1}^1 + U_{i,i+1}^2 + U_{i,i+1}^3 \quad (23)$$

with

$$U^1 = |\square q_1\rangle \langle 0q_0| + |\tilde{\square} q_1\rangle \langle 1q_0|, \quad (24)$$

$$U^2 = |q_2 1\rangle \langle q_1 0| + |q_2 0\rangle \langle q_1 1|, \quad (25)$$

$$U^3 = |1q_1\rangle \langle q_2 1| + |0q_1\rangle \langle q_2 0|, \quad (26)$$

which correspond to the transition rules 1,2,3, respectively. The quantum isometry of the total system is given by

$$U = \sum_i U_{i,i+1}. \quad (27)$$

The initial state is restricted to the form that only a single site takes $|q_0\rangle$ and other sites are in the local Hilbert subspace spanned by $\{|0\rangle, |1\rangle\}$, which ensures the emulation of legal states of the classical machine. Let $|\psi_n\rangle$ denote the state representing the state of the classical machine at the n -th step, then

$$U |\psi_n\rangle = |\psi_{n+1}\rangle \quad (28)$$

is satisfied, which means that the quantum isometry U induces evolution of the quantum state one step.

7.2 Construction of quantum partial isometry for M_G

Now we consider our original Turing machines. By defining

$$X := Q \cup Q_r \cup \{\bar{\Gamma} \times \Gamma_A\}, \quad (29)$$

$\mathbf{x} = (x_1, x_2, \dots, x_L)$ ($x_i \in X$) represents an instantaneous configuration of the generalized RTM M_G , where only one of x_i 's is a member of $Q \cup Q_r$. The last condition ensures the fact there is a single finite control and a single tape head in the system.

We denote by \mathcal{H}^X the Hilbert space spanned by $\{|x\rangle | x \in X\}$, and define \mathcal{H}^Q , \mathcal{H}^{Q_m} , \mathcal{H}^{Q_u} , \mathcal{H}^{Q_r} , $\mathcal{H}^{\bar{\Gamma}}$ and \mathcal{H}^{Γ_A} in a similar manner, which satisfy

$$\mathcal{H}^X = \mathcal{H}^Q \oplus \mathcal{H}^{Q_r} \oplus (\mathcal{H}^{\bar{\Gamma}} \otimes \mathcal{H}^{\Gamma_A}), \quad (30)$$

$$\mathcal{H}^Q = \mathcal{H}^{Q_m} \otimes \mathcal{H}^{Q_u}. \quad (31)$$

A quantum state $|\mathbf{x}\rangle \in (\mathcal{H}^X)^{\otimes L}$ represents \mathbf{x} , a configuration of M_G . Since we can choose a CONS arbitrarily in Lemma 1, we in particular employ the CONS $\{|x\rangle | x \in X\}$ and set as

$$|e_0\rangle = |m_0, q_0\rangle, \quad (32)$$

$$|e_i\rangle = |s_1, a_i\rangle, \quad (i = 1, 2). \quad (33)$$

Throughout this section, we suppose

$$\langle e_1 | A | e_1 \rangle = \langle s_1, a_1 | A | s_1, a_1 \rangle = 0, \quad (34)$$

$$\langle e_2 | A | e_2 \rangle = \langle s_1, a_2 | A | s_1, a_2 \rangle > 0. \quad (35)$$

Each step of the move (time evolution) of M_G can be described by a partial isometry acting on at most two sites simultaneously. Thus, the sum of the partial isometries acting on at most two sites properly emulates the time evolution of M_G . Suppose that in M_G the tape head is at the i -th cell, or equivalently $x_i \in Q \cup Q_r$. We set the partial isometry U_i acting on the $i - 1$, i , and $i + 1$ -th sites as

$$U_i = U_i^0 + U_i^{1+} + U_i^{1-} + U_i^{10} + U_i^r, \quad (36)$$

where each summand acts on at most two sites. If the state of the finite control is in (m_0, q) , the move of the machine is emulated by U_i^0 , which is an isometry from $\mathbb{C}(|m_0\rangle \otimes \mathcal{H}^{Q_u})_i \otimes (\mathcal{H}^{\bar{\Gamma}} \otimes \mathcal{H}^{\Gamma_A})_{i+1}$ to the same Hilbert space $\mathbb{C}(|m_0\rangle \otimes \mathcal{H}^{Q_u})_i \otimes (\mathcal{H}^{\bar{\Gamma}} \otimes \mathcal{H}^{\Gamma_A})_{i+1}$. If the i -th and $i + 1$ -th cell in M_G evolves from (x_i, x_{i+1}) to (x'_i, x'_{i+1}) , the corresponding isometry on the sites i and $i + 1$ is given by $|x'_i, x'_{i+1}\rangle \langle x_i, x_{i+1}|$. If the state of the finite control is in (m_1, q) , the move is emulated by one of U_i^{1+} , U_i^{1-} , or U_i^{10} , depending on whether $q \in Q_+$, Q_- , or Q_0 . They swaps the sites and change m_1 to m_0 . U_i^r mimics the move in the case that the state is $r \in Q_r$ and the finite control is at i -th site.

We note that if the i -th site does not corresponds to the finite control (i.e., $x_i \notin Q \cup Q_r$), then $U_i |\mathbf{x}\rangle = 0$, which ensures the fact that only the vicinity of the finite control can change. Owing to this, the isometry on $(\mathcal{H}^X)^{\otimes L}$ given by

$$U = \sum_i U_i \quad (37)$$

properly emulates the dynamics of the generalized RTM M_G .

8 Proof of Lemma 1: (3) Evaluating \bar{A} for computational basis state

8.1 General expression of long-time average

We first derive a general expression of the long-time average \bar{A} . Let H be a Hamiltonian of the system, and E_i and $|E_i\rangle$ be eigenenergy and corresponding energy eigenstate. We expand the initial state $|\psi\rangle$ with the energy eigenbasis as $|\psi\rangle = \sum_i c_i |E_i\rangle$. Then, the long-time average of an observable A is calculated as

$$\begin{aligned} \bar{A} &= \lim_{T \rightarrow \infty} \frac{1}{T} \int_0^T dt \langle \psi(t) | A | \psi(t) \rangle \\ &= \lim_{T \rightarrow \infty} \frac{1}{T} \int_0^T dt \sum_{i,j} e^{-i(E_j - E_i)t} \langle E_i | A | E_j \rangle \\ &= \sum_{i,j} \chi(E_j = E_i) \langle E_i | A | E_j \rangle, \end{aligned} \quad (38)$$

where $\chi(E_j = E_i)$ takes 1 if $E_j = E_i$ and takes zero otherwise. We set the Planck constant to unity. In the third line, we used the fact that $\lim_{T \rightarrow \infty} \frac{1}{T} \int_0^T dt e^{-i(E_j - E_i)t}$ converges to zero if $E_j \neq E_i$ and equal to 1 if $E_j = E_i$.

In particular, if the Hamiltonian H has no degeneracy, we have a simple expression $\bar{A} = \sum_i \langle E_i | A | E_i \rangle$. In contract, if there exist degeneracy ($E_i = E_j$ with $i \neq j$), we need to handle off-diagonal elements $\langle E_i | A | E_j \rangle$.

8.2 Hamiltonian emulating M_G and effective Hamiltonian

We now construct the Hamiltonian of the quantum system emulating M_G . We define the Hamiltonian as

$$H = \sum_i (U_i + U_i^\dagger), \quad (39)$$

where U_i is introduced in Eq. (36).

Let \mathbf{x}^j be the configuration of M_G at the j -th step, and J be the number of time steps until the machine stops. Then, its corresponding quantum state $|\mathbf{x}^j\rangle$ satisfies

$$|\mathbf{x}^j\rangle = U^{j-1} |\mathbf{x}^1\rangle, \quad (40)$$

and our Hamiltonian restricted to the Hilbert space spanned by $\{\mathbf{x}^i\}_{i=1}^J$ can be expressed as

$$H_{\text{eff}} := \sum_{j=1}^{J-1} |\mathbf{x}^{j+1}\rangle \langle \mathbf{x}^j| + \text{h.c.} \quad (41)$$

Note that \mathbf{x}^J does not have a successor, and hence the evolution of M_G stops at this point.

Since H_{eff} is a tridiagonal matrix with the basis $\{|\mathbf{x}^i\rangle\}_{i=1}^J$, we can fully solve its eigenenergies and eigenstates. The k -th eigenenergy is written as

$$E_k = 2 \cos \left(\frac{k\pi}{J+1} \right) \quad (42)$$

($k = 1, 2, \dots, J$) with the corresponding energy eigenstate

$$|E_k\rangle = \sqrt{\frac{2}{J+1}} \sum_{j=1}^J \sin \left(\frac{kj\pi}{J+1} \right) |\mathbf{x}^j\rangle. \quad (43)$$

Note that $0 < \frac{k\pi}{J+1} < \pi$ guarantees absence of degeneracy in this Hamiltonian.

8.3 Computing long-time average of A

The initial state $|\mathbf{x}^1\rangle$ is expanded by the energy eigenstates as

$$|\mathbf{x}^1\rangle = \sqrt{\frac{2}{J+1}} \sum_{k=1}^J \sin \left(\frac{k\pi}{J+1} \right) |E_k\rangle, \quad (44)$$

and thus \bar{A} is calculated as

$$\begin{aligned}
\bar{A} &= \frac{2}{J+1} \sum_{k=1}^J \sin^2 \left(\frac{k\pi}{J+1} \right) \langle E_k | A_L | E_k \rangle \\
&= \left(\frac{2}{J+1} \right)^2 \sum_{j,j'=1}^J \left[\sum_{k=1}^J \sin^2 \left(\frac{k\pi}{J+1} \right) \sin \frac{j'k\pi}{J+1} \sin \frac{jk\pi}{J+1} \right] \langle \mathbf{x}^j | A_L | \mathbf{x}^{j'} \rangle \\
&= \frac{3}{2(J+1)} (\langle \mathbf{x}^1 | A_L | \mathbf{x}^1 \rangle + \langle \mathbf{x}^J | A_L | \mathbf{x}^J \rangle) + \frac{1}{J+1} \sum_{j=2}^{J-1} \langle \mathbf{x}^j | A_L | \mathbf{x}^j \rangle - \frac{1}{2(J+1)} \sum_{\substack{1 \leq j, j' \leq J \\ j=j' \pm 2}} \langle \mathbf{x}^j | A_L | \mathbf{x}^{j'} \rangle.
\end{aligned} \tag{45}$$

Here, in the first line we used Eq. (38), and in the last line we used the following relation:

$$\sum_{k=1}^J \sin^2 \left(\frac{k\pi}{J+1} \right) \sin \frac{j'k\pi}{J+1} \sin \frac{jk\pi}{J+1} = \begin{cases} \frac{1}{4}(J+1) & j = j' \neq 1 \text{ and } \neq J, \\ \frac{3}{8}(J+1) & j = j' = 1 \text{ or } J, \\ 0 & j \neq j' \text{ and } j \neq j' \pm 2, \\ -\frac{1}{8}J(J+1) & j = j' \pm 2. \end{cases} \tag{46}$$

Now, we shall show that the last term $\langle \mathbf{x}^j | A_L | \mathbf{x}^{j'} \rangle$ is sufficiently small. Observe that $\mathbf{x}^j \neq \mathbf{x}^{j'}$ and A_L is a sum of one-body observables; $A_L = \frac{1}{L} \sum_i A_i$. Hence, $\langle \mathbf{x}^j | A_L | \mathbf{x}^{j'} \rangle$ can take a nonzero value only if \mathbf{x}^j and $\mathbf{x}^{j'}$ differs only in a single site. By denoting this site by i^* , we bound the last term $\langle \mathbf{x}^j | A_L | \mathbf{x}^{j'} \rangle$ as

$$\left| \langle \mathbf{x}^j | A_L | \mathbf{x}^{j'} \rangle \right| = \frac{1}{L} \left| \sum_{i=1}^L \langle \mathbf{x}^j | A_i | \mathbf{x}^{j'} \rangle \right| = \frac{1}{L} \left| \langle \mathbf{x}^j | A_{i^*} | \mathbf{x}^{j'} \rangle \right| \leq \frac{1}{L} \|A\|. \tag{47}$$

Thus, the last term of Eq. (45) is bounded above as

$$\left| \frac{1}{2(J+1)} \sum_{\substack{1 \leq j, j' \leq J \\ j=j' \pm 2}} \langle \mathbf{x}^j | A_L | \mathbf{x}^{j'} \rangle \right| \leq \left| \frac{1}{2(J+1)} \sum_{\substack{1 \leq j, j' \leq J \\ j=j' \pm 2}} \frac{1}{L} \|A\| \right| = \frac{J-2}{J+1} \frac{1}{L} \|A\|, \tag{48}$$

whose right-hand side vanishes in the $L \rightarrow \infty$ limit. Therefore, in the following we dropped this term for brevity.

We finally evaluate the first two terms of Eq. (45). Let $N_A(\mathbf{x}^j)$ be the number of A-cells in \mathbf{x}^j filled with a_2 . Then, we have

$$\left| \langle \mathbf{x}^j | A_L | \mathbf{x}^j \rangle - \frac{N_A(\mathbf{x}^j)}{L} \langle e_2 | A | e_2 \rangle \right| \leq \alpha \|A\|, \tag{49}$$

where the difference between $\langle \mathbf{x}^j | A_L | \mathbf{x}^j \rangle$ and $\frac{N_A(\mathbf{x}^j)}{L} \langle e_2 | A | e_2 \rangle$ comes from the presence of M-cells. In case of halting, by taking L sufficiently large, we can make M_G halt before $J/2$

steps. In this condition, $\frac{N_A(\mathbf{x}^j)}{L} \geq 2(j - \frac{J}{2})$ is satisfied for $j \geq \frac{J}{2}$, which indicates

$$\bar{A} = \frac{3}{2(J+1)} (\langle \mathbf{x}^1 | A_L | \mathbf{x}^1 \rangle + \langle \mathbf{x}^J | A_L | \mathbf{x}^J \rangle) + \frac{1}{J+1} \sum_{j=2}^{J-1} \langle \mathbf{x}^j | A_L | \mathbf{x}^j \rangle \geq \frac{1}{4} \langle e_2 | A | e_2 \rangle - \alpha \|A\|. \quad (50)$$

By taking α sufficiently small, we arrive at the relation $\bar{A} \geq (\frac{1}{4} - \eta) \langle e_2 | A | e_2 \rangle$ in case of halting.

In case of non-halting, since $N_A(\mathbf{x}^j) = 0$ for any j , we have

$$\bar{A} = \frac{3}{2(J+1)} (\langle \mathbf{x}^1 | A_L | \mathbf{x}^1 \rangle + \langle \mathbf{x}^J | A_L | \mathbf{x}^J \rangle) + \frac{1}{J+1} \sum_{j=2}^{J-1} \langle \mathbf{x}^j | A_L | \mathbf{x}^j \rangle \leq \alpha \|A\|. \quad (51)$$

By taking α sufficiently small, we arrive at the relation $\bar{A} \leq \eta$ in case of non-halting.

9 Proof of Lemma 1: (4) Evaluating \bar{A} for superposition of computational basis states

9.1 Setting of the initial state and decoding of the input

We now consider our original setting where the initial state is shift-invariant except the first site, which takes the form of

$$|\psi_{V,L}\rangle = (V |e_0\rangle) \otimes (V |e_1\rangle)^{\otimes L-1} = |e_0\rangle \otimes (V |e_1\rangle)^{\otimes L-1}. \quad (52)$$

Here, $|e_0\rangle$ represents the state corresponding to the initial state of the finite control, and others represent cells. In particular, $\langle e_0 | V | e_1 \rangle = \langle e_0 | e_1 \rangle = 0$ is satisfied.

To encode the input for TM2, we elongate the local Hilbert subspace to $\mathcal{H}^{\bar{\Gamma}} \otimes \mathcal{H}^{\Gamma_A} \otimes \mathcal{H}^{\text{in}}$. The input for TM2 is encoded into $|\psi_{\text{in}}\rangle \in \{|0\rangle, |1\rangle\}^{\otimes 2} \subset \mathcal{H}^{\text{in}}$, which sits in all M-cells. If the cell is an A-cell, this part is blank (constant independent of the input), $|\psi_0\rangle \in \mathcal{H}^{\text{in}}$ say. The Hilbert space \mathcal{H}^{in} is a 5-dimensional space which is a sum of a 2 q-bit space and a single state space $\{|\psi_0\rangle\}$:

$$\mathcal{H}^{\text{in}} = \text{span}\{(|0\rangle, |1\rangle)^{\otimes 2} \oplus |\psi_0\rangle\}. \quad (53)$$

The input is decoded by an additional reversible Turing machine called TM1.

In the previous section, we set αL cells to M-cells and $(1 - \alpha)L$ cells to A-cells. In this section, instead of this, we set $V |e_1\rangle$ as a superposition of these two types of cells. We first set $|e_1\rangle$ and $|e_2\rangle$ as

$$|e_k\rangle := |s_1, a_k\rangle |\psi_0\rangle, \quad (k = 1, 2), \quad (54)$$

and then set the operator V which slightly rotates $|e_k\rangle$ ($k = 1, 2$) such that

$$V |e_k\rangle = \sqrt{\alpha} |s_0, a_k\rangle |\psi_{\text{in}}\rangle + \sqrt{1 - \alpha} |e_k\rangle \in \mathcal{H}^{\bar{\Gamma}} \otimes \mathcal{H}^{\Gamma_A} \otimes \mathcal{H}^{\text{in}}. \quad (55)$$

Here, two states, $|s_0, a_k\rangle |\psi_{\text{in}}\rangle$ and $|e_k\rangle = |s_1, a_k\rangle |\psi_0\rangle$, correspond to an M-cell and an A-cell, respectively. The symbol s_0 serves as a blank cell of M-cells in the first layer, and $|\psi_{\text{in}}\rangle \in \mathcal{H}^{\text{in}}$ stores the input for TM2 in the second and third layers of M-cells. In $|s_0, a_k\rangle |\psi_{\text{in}}\rangle$, the symbol a_k plays no role. In $|s_1, a_k\rangle |\psi_0\rangle$, the symbol s_1 is a sign to be A-cells, and $|\psi_0\rangle$ is

some state whose details are not important in the following discussion. We set the operator V as an identity operator on the orthogonal component of $\mathcal{H}^{\Gamma} \otimes \mathcal{H}^{\Gamma^A} \otimes \mathcal{H}^{\text{in}}$. In particular, V stabilizes $|e_0\rangle$ (i.e., $V|e_0\rangle = |e_0\rangle$).

The state $|\psi_{\text{in}}\rangle$ takes the form of

$$|\psi_{\text{in}}\rangle = (\sqrt{\beta}|1\rangle + \sqrt{1-\beta}|0\rangle) \otimes (\sqrt{\gamma}|1\rangle + \sqrt{1-\gamma}|0\rangle), \quad (56)$$

where the binary expansion of β is set to be equal to the input for TM2 in the form of binary bit string. To determine the end of the input code uniquely, we employ a prefix-free code⁴ as the input for TM2. The amount of β is guessed by the relative frequency of 1's in the second layer (see also Fig. 1.(a)). The second layer is a superposition of computational basis states, and TM1 runs in each computational basis states as a quantum superposition. Consider m copies of $\sqrt{\beta}|1\rangle + \sqrt{1-\beta}|0\rangle$, which is expanded as

$$(\sqrt{\beta}|1\rangle + \sqrt{1-\beta}|0\rangle)^{\otimes m} = \sum_{\mathbf{w} \in \{0,1\}^{\otimes m}} \sqrt{\beta}^{N_1(\mathbf{w})} \sqrt{1-\beta}^{m-N_1(\mathbf{w})} |\mathbf{w}\rangle. \quad (57)$$

Here, $N_1(\mathbf{w})$ is the number of 1's in the binary sequence \mathbf{w} . The probability amplitude for a computational basis state $|\mathbf{w}\rangle$ is $|c_{\mathbf{w}}|^2 = \beta^{N_1(\mathbf{w})} (1-\beta)^{m-N_1(\mathbf{w})}$. Due to the law of large numbers, the probability amplitude for states with relative frequency of 1's close to β converges to 1 in the large m limit:

$$\lim_{m \rightarrow \infty} \sum_{\mathbf{w}: \frac{N_1(\mathbf{w})}{m} \simeq \beta} |c_{\mathbf{w}}|^2 = 1, \quad (58)$$

where the precise meaning of the symbol $\frac{N_1(\mathbf{w})}{m} \simeq \beta$ is clarified soon later (in Eq. (60)). Hence, if m is sufficiently large compared with the length of the input code, n say, TM1 guesses β correctly from the frequency of 1's.

The length of q-bit m is determined by another bit sequence $\sqrt{\gamma}|1\rangle + \sqrt{1-\gamma}|0\rangle$ in the third layer. For any given accuracy $0 < \xi < 1$, the information of m is encoded to γ as satisfying

$$(1-\gamma)^m \geq 1-\xi. \quad (59)$$

Here, γ is set to extremely close to 0, and thus almost all q-bits are $|0\rangle$ in this sequence and $|1\rangle$ rarely appears. In particular, $|1\rangle$ appears only after m -th digit with probability larger than $1-\xi$. Owing to this, if $|1\rangle$ appears at the m' -th digit for the first time, this is taken as the sign that $m \leq m'$. Based on the observed value m' , the length of the output by TM1 (i.e., the presumed length of the digit of β) is determined as $n' = \lceil \frac{1}{4} \log_2 m \rceil$, which ensures

$$\lim_{m \rightarrow \infty} \text{Prob} \left[\left| \frac{N_1(\mathbf{w})}{m} - \beta \right| < \frac{1}{2^{n'+1}} \right] = 1. \quad (60)$$

With the choice of this output length n' , guessing m larger than the true value does not affect the correctness of the estimation of β .

The composition of TM1, TM2, and TM3 is represented by a generalized RTM \tilde{M}_G , which is constructed in parallel with M_G . The state space of the finite control of \tilde{M}_G is $(Q_m \times (Q_u \cup Q_{\text{dec}})) \cup Q_r$, where Q_{dec} is the state space of the finite control of TM1. Let \tilde{Q}_u

⁴A simple example is a code $00 \rightarrow 0$ and $11 \rightarrow 1$. We promise that the code 01 and 10 are a signal of the end.

denote $Q_u \cup Q_{\text{dec}}$ in this section. The tape alphabet is also extended as $\bar{\Gamma} \times \Gamma_A \times \Gamma_{\text{in}}$. In this setting, the configuration of \tilde{M}_G is represented by the sequence of \mathbf{x} with $x_i \in \tilde{X}$ with length $L + 1$, where we defined

$$\tilde{X} := (Q_m \times Q_u) \cup Q_r \cup (\bar{\Gamma} \times \Gamma_A \times \Gamma_{\text{in}}). \quad (61)$$

Using them, we construct the corresponding Hilbert spaces, local isometries \tilde{U}_i , the total isometry as

$$\tilde{U} := \sum_i \tilde{U}_i, \quad (62)$$

and the total Hamiltonian as

$$\tilde{H} := \tilde{U} + \tilde{U}^\dagger \quad (63)$$

in a similar manner to the previous section.

9.2 Case when TM2 halts 1: decoding and expression of states

Suppose that TM2 halts on the encoded input. We claim that in this case with overwhelming probability amplitude the dynamics by \tilde{U} before halting is described by the configuration of the first L_0 of M-cells with sufficiently large L_0 in the following sense:

- It is not smaller than the space used by TM1 and TM2.
- It should be large enough to encounter at least a single $|1\rangle$ in the third layer in the first L_0 of M-cells with high probability. In other words, for a given $0 < \xi, \xi' < 1$ we set γ and L_0 such that

$$\begin{aligned} (1 - \gamma)^m &\geq 1 - \xi, \\ (1 - \gamma)^{L_0} &\leq 1 - \xi', \end{aligned} \quad (64)$$

where the first line is the same as Eq. (59). With these conditions, the first $|1\rangle$ in the second layer appears between the first m of M-cells and the first L_0 of M-cells with high probability.

Let C be the cluster of the first $|C|$ sites with

$$|C| = \frac{L_0}{\alpha} + o(L_0). \quad (65)$$

Here, the $o(L_0)$ term is chosen so that C contains at least L_0 of M-cells with high probability. The cells not in the cluster C may interact with the finite control only when $q \in Q_r$, which means that only Γ_A -parts may be touched. This fact motivates the following representation of the initial state: Let \mathbf{y} be the first $|C|$ components of \mathbf{x} , that is, the configuration of sites in the cluster C , and also denote by Y the set of all possible \mathbf{y} 's. Then, the initial state of the total system can be expressed as

$$|\psi_{V,L}\rangle = \sum_{\mathbf{y} \in Y} c_{\mathbf{y}} |\mathbf{y}\rangle \otimes (V |e_1\rangle)^{\otimes L - |C|}. \quad (66)$$

We call \mathbf{y} “good” initial configurations if (i) the input for TM2 is correctly decoded by TM1, and (ii) in the dynamics induced by the isometry \tilde{U} the finite control does not come

out from the cluster C before the simulation of TM2 reaches the halting state. We write as Y^* the set of good initial configurations in the above sense, and define the following unnormalized state:

$$|\psi_{V,L}^*\rangle := \sum_{\mathbf{y} \in Y^*} c_{\mathbf{y}} |\mathbf{y}\rangle \otimes (V|e_1\rangle)^{\otimes L-|C|}. \quad (67)$$

The dynamics starting from $|\psi_{V,L}^*\rangle$ and $|\psi_{V,L}\rangle$ are arbitrarily close because the trace norm between the states $|\psi_{V,L}^*(t)\rangle = e^{-i\tilde{H}t} |\psi_{V,L}^*\rangle$ and $|\psi_{V,L}(t)\rangle = e^{-i\tilde{H}t} |\psi_{V,L}\rangle$ is bounded as

$$\begin{aligned} \|\psi_{V,L}^*(t)\rangle \langle \psi_{V,L}^*(t)| - |\psi_{V,L}(t)\rangle \langle \psi_{V,L}(t)|\|_1 &= \|\psi_{V,L}^*\rangle \langle \psi_{V,L}^*| - |\psi_{V,L}\rangle \langle \psi_{V,L}|\|_1 \\ &\leq 2\sqrt{1 - \left|\langle \psi_{V,L} | \psi_{V,L}^* \rangle\right|^2} \leq 2\sqrt{4\xi} = 4\sqrt{\xi}. \end{aligned} \quad (68)$$

Note that ξ can be arbitrarily small, and therefore, in the following we regard $|\psi^*\rangle$ as the initial state itself.

For each good initial configuration \mathbf{y} , we define the j -th state as

$$|j, \mathbf{y}\rangle := \tilde{U}^{j-1} |\mathbf{y}\rangle \otimes (V|e_1\rangle)^{\otimes L-|C|}. \quad (69)$$

Recalling that \tilde{U} updates the Γ -part of the M-cell in simulating TM1 and TM2, and Γ_A part after the halting, we find that \tilde{U} either changes \mathbf{y} into another configuration \mathbf{y}' , or interchanges $V|e_k\rangle$'s ($k = 1, 2$). The above observation implies that $|j, \mathbf{y}\rangle$ is written in the form of

$$|j, \mathbf{y}\rangle = |\mathbf{y}'\rangle \otimes (\otimes_{i=|C|+1}^L V|e_{k_i}\rangle), \quad (70)$$

where $k_i = 1, 2$. This confirms that two states at different steps with the same initial state are orthogonal:

$$\langle j, \mathbf{y} | j', \mathbf{y} \rangle = 0 \quad (71)$$

for any $j \neq j'$.

9.3 Case when TM2 halts 2: long-time average of A

Using the eigenenergies and eigenstates shown in Eqs. (42) and (43), $e^{-i\tilde{H}t} |1, \mathbf{y}\rangle$ is computed as

$$\begin{aligned} e^{-i\tilde{H}t} |1, \mathbf{y}\rangle &= \sqrt{\frac{2}{J_{\mathbf{y}} + 1}} \sum_{k=1}^{J_{\mathbf{y}}} e^{-iE_{k,\mathbf{y}}t} \sin \frac{k\pi}{J_{\mathbf{y}} + 1} |E_{k,\mathbf{y}}\rangle \\ &= \frac{2}{J_{\mathbf{y}} + 1} \sum_{k=1}^{J_{\mathbf{y}}} e^{-iE_{k,\mathbf{y}}t} \sin \frac{k\pi}{J_{\mathbf{y}} + 1} \sum_{j=1}^{J_{\mathbf{y}}} \sin \frac{jk\pi}{J_{\mathbf{y}} + 1} |j, \mathbf{y}\rangle, \end{aligned} \quad (72)$$

where

$$E_{k,\mathbf{y}} := 2 \cos \frac{k\pi}{J_{\mathbf{y}} + 1}, \quad (73)$$

$$|E_{k,\mathbf{y}}\rangle := \sqrt{\frac{2}{J_{\mathbf{y}} + 1}} \sum_{j=1}^{J_{\mathbf{y}}} \sin \frac{jk\pi}{J_{\mathbf{y}} + 1} |j, \mathbf{y}\rangle \quad (74)$$

are the k -th energy eigenvalue and corresponding energy eigenstate of the effective Hamiltonian $H_{\text{eff}} = \sum_j |j+1, \mathbf{y}\rangle \langle j, \mathbf{y}| + \text{c.c.}$, and $J_{\mathbf{y}}$ is the number of states for the termination of \tilde{M}_G starting from the configuration in the cluster C as \mathbf{y} .

Using Eq. (38), the long-time average of A from the initial state $|\psi_{V,L}^*\rangle$ given in Eq. (67) is calculated as

$$\bar{A} = \sum_{k,k',\mathbf{y},\mathbf{y}'} \chi(E_{k,\mathbf{y}} = E_{k',\mathbf{y}'}) c_{\mathbf{y}}^* c_{\mathbf{y}'} \sqrt{\frac{2}{J_{\mathbf{y}}+1}} \sqrt{\frac{2}{J_{\mathbf{y}'}+1}} \sin \frac{k\pi}{J_{\mathbf{y}}+1} \sin \frac{k'\pi}{J_{\mathbf{y}'}+1} \langle E_{k,\mathbf{y}} | A_L | E_{k',\mathbf{y}'} \rangle, \quad (75)$$

where $\chi(E_{k,\mathbf{y}} = E_{k',\mathbf{y}'})$ takes 1 if $E_{k,\mathbf{y}} = E_{k',\mathbf{y}'}$ and takes zero otherwise. Since the contribution from the case of $\mathbf{y} = \mathbf{y}'$ (diagonal elements) has already been calculated and shown to be a finite amount in Sec. 8, it suffices to prove that the contribution to \bar{A} from the case of $\mathbf{y} \neq \mathbf{y}'$ (off-diagonal elements) is sufficiently small.

The form of Eq. (73) directly implies that the condition $E_{k,\mathbf{y}} = E_{k',\mathbf{y}'}$ can be written as

$$\frac{k}{k'} = \frac{J_{\mathbf{y}}+1}{J_{\mathbf{y}'}+1}. \quad (76)$$

Let G be the greatest common divisor of $J_{\mathbf{y}}+1$ and $J_{\mathbf{y}'}+1$, and define $k_0 := \frac{J_{\mathbf{y}}+1}{G}$ and $k'_0 := \frac{J_{\mathbf{y}'}+1}{G}$. Then, k and k' with Eq. (76) are expressed as $k = lk_0$ and $k' = lk'_0$ with $l = 1, 2, \dots, G$, and thus

$$\frac{k}{J_{\mathbf{y}}+1} = \frac{k'}{J_{\mathbf{y}'}+1} = \frac{l}{G} \quad (77)$$

is satisfied. Hence, for any $\mathbf{y} \neq \mathbf{y}'$ we have

$$\begin{aligned} & \sum_{\substack{k,k' \\ E_{k,\mathbf{y}}=E_{k',\mathbf{y}'}}} \sin \frac{k\pi}{J_{\mathbf{y}}+1} \sin \frac{k'\pi}{J_{\mathbf{y}'}+1} \langle E_{k,\mathbf{y}} | A_L | E_{k',\mathbf{y}'} \rangle \\ &= \sum_{l=1}^{G-1} \sin^2 \frac{l\pi}{G} \langle E_{lk_0l,\mathbf{y}} | A_L | E_{lk'_0l,\mathbf{y}'} \rangle \\ &= \sqrt{\frac{2}{J_{\mathbf{y}}+1}} \sqrt{\frac{2}{J_{\mathbf{y}'}+1}} \sum_{l=1}^G \sum_{j=1}^{J_{\mathbf{y}}} \sum_{j'=1}^{J_{\mathbf{y}'}} \sin \frac{j l \pi}{G} \sin \frac{j' l \pi}{G} \sin^2 \frac{l\pi}{G} \langle j, \mathbf{y} | A_L | j', \mathbf{y}' \rangle \\ &= \frac{1}{4} \sqrt{\frac{2}{J_{\mathbf{y}}+1}} \sqrt{\frac{2}{J_{\mathbf{y}'}+1}} \sum_{l=1}^G \sum_{j=1}^{J_{\mathbf{y}}} \sum_{j'=1}^{J_{\mathbf{y}'}} \left(\cos \frac{(j+j')l\pi}{G} + \cos \frac{(j-j')l\pi}{G} \right) \left(1 - \cos \frac{2l\pi}{G} \right) \langle j, \mathbf{y} | A_L | j', \mathbf{y}' \rangle \\ &\leq \frac{1}{2} \sqrt{\frac{2}{J_{\mathbf{y}}+1}} \sqrt{\frac{2}{J_{\mathbf{y}'}+1}} \sum_{l=1}^G \sum_{j=1}^{J_{\mathbf{y}}} \sum_{j'=1}^{J_{\mathbf{y}'}} \left(\cos \frac{(j+j')l\pi}{G} + \cos \frac{(j-j')l\pi}{G} \right) \langle j, \mathbf{y} | A_L | j', \mathbf{y}' \rangle \\ &\leq \frac{1}{2} \sqrt{\frac{2}{J_{\mathbf{y}}+1}} \sqrt{\frac{2}{J_{\mathbf{y}'}+1}} (J_{\mathbf{y}}+1)(J_{\mathbf{y}'}+1) \langle j, \mathbf{y} | A_L | j', \mathbf{y}' \rangle \\ &\leq \sqrt{(J_{\mathbf{y}}+1)(J_{\mathbf{y}'}+1)} \frac{\|A\|}{L}. \end{aligned} \quad (78)$$

In the sixth line, we used the fact that $\sum_{l=1}^G \cos \frac{(j+j')l\pi}{G}$ is equal to G if $j+j'$ is a multiple of $2G$ and is equal to zero otherwise. In the seventh line, we used the following relation

similar to Eq. (47)

$$|\langle j, \mathbf{y} | A_L | j', \mathbf{y}' \rangle| = \left| \frac{1}{L} \sum_{i=1}^L \langle j, \mathbf{y} | A_i | j', \mathbf{y}' \rangle \right| \leq \frac{\|A\|}{L} \quad (79)$$

for any $\mathbf{y} \neq \mathbf{y}'$. As is the case of Eq. (47), this relation follows from the fact that the configurations (j, \mathbf{y}) and (j', \mathbf{y}') differs at least a single site.

Substituting Eq. (78) into Eq. (75) in case of $\mathbf{y} \neq \mathbf{y}'$, we arrive at the upper bound for the off-diagonal sum:

$$\begin{aligned} & \left| \sum_{\substack{k, k', \mathbf{y}, \mathbf{y}' \\ \mathbf{y} \neq \mathbf{y}'}} \chi(E_{k, \mathbf{y}} = E_{k', \mathbf{y}'}) c_{\mathbf{y}}^* c_{\mathbf{y}'} \sqrt{\frac{2}{J_{\mathbf{y}} + 1}} \sqrt{\frac{2}{J_{\mathbf{y}'} + 1}} \sin \frac{k\pi}{J_{\mathbf{y}} + 1} \sin \frac{k'\pi}{J_{\mathbf{y}'} + 1} \langle E_{k, \mathbf{y}} | A_L | E_{k', \mathbf{y}'} \rangle \right| \\ & \leq \frac{2\|A\|}{L} \sum_{\mathbf{y} \neq \mathbf{y}'} |c_{\mathbf{y}}^* c_{\mathbf{y}'}| \leq \frac{2\|A\|}{L} \left(\sum_{\mathbf{y}} |c_{\mathbf{y}}| \right)^2 \leq \frac{2\|A\|}{L} |Y^*|. \end{aligned} \quad (80)$$

Notably, $|Y^*|$ is independent of the total system size L , and hence, by taking the thermodynamic limit $L \rightarrow \infty$ the right-hand side becomes arbitrarily small. Thus, using the result in Sec. 8, we have

$$\bar{A} \geq \frac{1}{4} \langle e_2 | A | e_2 \rangle - \alpha \|A\| \quad (81)$$

and

$$\overline{VAV^\dagger} \geq \frac{1}{4} \langle e_2 | VAV^\dagger | e_2 \rangle - \alpha \|A\| \geq \frac{1-\alpha}{4} \langle e_2 | A | e_2 \rangle - 2(\alpha + \sqrt{\alpha(1-\alpha)}) \|A\|. \quad (82)$$

By taking α sufficiently small, we arrive at the desired result

$$\min\{\bar{A}, \overline{VAV^\dagger}\} \geq \frac{1-\alpha}{4} \langle e_2 | A | e_2 \rangle - 2(\alpha + \sqrt{\alpha(1-\alpha)}) \|A\| \geq \left(\frac{1}{4} - \eta\right) \langle e_2 | A | e_2 \rangle \quad (83)$$

for any $\eta > 0$.

9.4 Case when TM2 does not halt

In this subsection, we consider the case that TM2 does not halt with the decoded input. To bound the off-diagonal elements from above, we need a completely different treatment from the case of halting, because the size of the cluster C now becomes the entire system (The cluster C should contain the working space of TM2, which is unlimited in case of non-halting).

In order to treat the non-halting case, we focus on the fact that most of the cells in the initial state is A-cells. By construction, the number of A-cells is invariant under the time evolution, and if the decoding of input succeeds, all the A-cells are filled with the symbol a_1 at all times.

We first restrict the state space to “good” configurations of \mathbf{x} . In this subsection, we employ the word “good” initial configurations with a slightly different definition from the previous subsection. We say that \mathbf{x} is a “good” initial configuration if (i) the input for TM2 is correctly decoded by TM1, and (ii) the fraction of A-cells is larger than $1 - \alpha'$, where α' is set properly as slightly larger than but close to α . We do not require the size of the

working space for TM2. We write as X^* the set of good initial configurations in the above sense, and define the following unnormalized state:

$$|\psi_L^{**}\rangle := \sum_{\mathbf{x} \in X^*} c_{\mathbf{x}} |\mathbf{x}\rangle. \quad (84)$$

For a similar reason to the case of Y^* and $|\psi_{V,L}^*\rangle$, the dynamics starting from $|\psi_L^{**}\rangle$ denoted by $|\psi_L^{**}(t)\rangle$ is arbitrarily close to the actual dynamics $|\psi_L(t)\rangle$. Therefore, in the following we consider the state $|\psi_L^{**}(t)\rangle$ instead of the actual one.

Let $P := |e_1\rangle\langle e_1|$ be the projector onto the A-cell filled with the symbol a_1 , and P_i be the aforementioned projector acting on the i -th site. If $|\mathbf{x}\rangle$ represents a configuration of \tilde{M}_G , $\text{Tr}[P_i |\mathbf{x}\rangle\langle \mathbf{x}|]$ equals 1 (resp. 0) iff the i -th cell is (resp. is not) an A-cell with the symbol a_1 . Hence, we have

$$\text{Tr}\left[\sum_{i=1}^{L+1} P_i |\psi_L^{**}(t)\rangle\langle \psi_L^{**}(t)|\right] \geq (1 - \alpha')L \quad (85)$$

for any t . Let $\rho_i(t)$ denote the reduced density operator of $|\psi_L^{**}(t)\rangle\langle \psi_L^{**}(t)|$ onto the i -th site, and define the averaged density operator over all sites as

$$\bar{\rho}(t) := \frac{1}{L} \sum_{i=1}^L \rho_i(t). \quad (86)$$

Then, using a relation

$$\text{Tr}[P\bar{\rho}(t)] = \langle e_1 | \bar{\rho}(t) | e_1 \rangle \geq 1 - \alpha', \quad (87)$$

we arrive at the desired result:

$$\begin{aligned} |\langle \psi_L(t) | A_L | \psi_L(t) \rangle| &= |\langle \psi_L(t) | A_L | \psi_L(t) \rangle - \langle e_1 | A | e_1 \rangle| \\ &= |\text{Tr}[A\bar{\rho}(t)] - \langle e_1 | A | e_1 \rangle| \\ &\leq \|\bar{\rho}(t) - |e_1\rangle\langle e_1|\|_1 \|A\| \\ &\leq 2\sqrt{1 - \frac{(1 - \alpha')L}{L+1}} \|A\| \\ &< 2\sqrt{\alpha'} \|A\|. \end{aligned} \quad (88)$$

We thus arrive at the desired relation $\bar{A} < 2\sqrt{2\alpha'} \|A\|$.

To show Lemma 1, we also need to evaluate the state with V rotation, which is evaluated as

$$\begin{aligned} &\left| \frac{1}{L} \langle \psi_L | V^{\otimes L} A_L V^{\dagger \otimes L} | \psi_L \rangle - \langle e_1 | A | e_1 \rangle \right| \\ &\leq \left| \frac{1}{L} \langle \psi_L | V^{\otimes L} A_L V^{\dagger \otimes L} | \psi_L \rangle - \langle e_1 | V A V^{\dagger} | e_1 \rangle \right| + \left| \langle e_1 | V A V^{\dagger} | e_1 \rangle - \langle e_1 | A | e_1 \rangle \right|. \end{aligned} \quad (89)$$

The first term has already been calculated in Eq. (88), which is bounded from above by

$2\sqrt{2\alpha}\|A\|$. The second term is calculated as

$$\begin{aligned} |\langle e_1|VAV^\dagger|e_1\rangle - \langle e_1|A|e_1\rangle| &\leq \|A\| |\langle e_1| - V^\dagger|e_1\rangle \langle e_1|V| \\ &= \|A\| \sqrt{1 - \langle e_1|V|e_1\rangle} \\ &= \|A\| \sqrt{\alpha}, \end{aligned} \quad (90)$$

where in the last line we used Eqs. (55) and (54). Combining them, we find

$$\max\{\bar{A}, \overline{VAV^\dagger}\} \leq 2\sqrt{\alpha}\|A\|, \quad (91)$$

whose right-hand side can become arbitrarily small by taking α sufficiently small. In particular, $\max\{\bar{A}, \overline{VAV^\dagger}\} \leq \eta$ is fulfilled.

10 Remarks

10.1 Dimension of the local Hilbert space

We have not discussed how large the sufficient dimension of the local Hilbert space is. Although we do not calculate it rigorously here, we present a rough estimation of it.

To reduce the dimension, it is useful to enlarge the tape alphabet. With more symbols the tape alphabet has, with less states the finite control needs to have. It has been established that there are URTMs with 10-state and 8-symbol, 15-state and 6-symbol, 24-state and 4-symbol, 32-state and 3-symbol, and 138-state and 2-symbol [64]. By employing the 24-state 4-symbol URTM, 24 states in the finite control and $(4+1) \times 2 \times 2^2 = 40$ symbols in the tape alphabet suffice for TM2 (see Fig. 2). Although we do not evaluate the sufficient number of states and symbols for TM1, since the tasks of TM1 are all elementary, counting the number of 1's and 0's and computing logarithm and division, we roughly estimate that 50 states and 4 symbols suffice for TM1. If the above estimation is correct, the sufficient dimension of the local Hilbert space is $(24 + 50 + 1) + (40 + 2 + 2) = 119$.

10.2 Exact value of \bar{A} in thermodynamic limit when TM2 halts

In the previous section, we only derive an inequality for the value of \bar{A} when TM2 halts. We here briefly calculate the value of \bar{A} in the thermodynamic limit when TM2 halts.

We start from Eq. (49) and the equality part of Eq. (50) for non-uniform (computational basis) initial states. By taking L to infinity, the number of steps before TM2 halts is negligibly small compared to the total number of steps J . Thus the right-hand side in the equality of Eq. (50) is calculated as

$$\frac{3}{2(J+1)} (\langle \mathbf{x}^1|A_L|\mathbf{x}^1\rangle + \langle \mathbf{x}^J|A_L|\mathbf{x}^J\rangle) + \frac{1}{J+1} \sum_{j=2}^{J-1} \langle \mathbf{x}^j|A_L|\mathbf{x}^j\rangle = \frac{1-\alpha}{2} \langle e_2|A|e_2\rangle \quad (92)$$

for computational basis initial states, where we assumed that M-cells and A-cells are uniformly distributed. By combining Eq. (49), this relation leads to the bound for \bar{A} for computational basis initial states: $|\bar{A} - \frac{1-\alpha}{2} \langle e_2|A|e_2\rangle| \leq \alpha\|A\|$. In case of uniform initial states (excepts the first site), we have already shown that off-diagonal terms and various other correction terms vanish in the thermodynamic limit. Thus, by using Eqs. (75) and

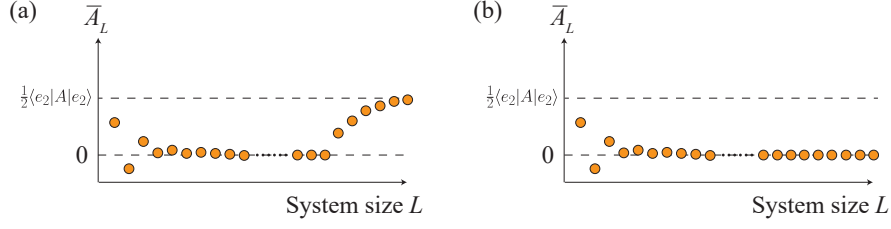


Figure 4: A possible situation in numerical exact diagonalization. Although the long-time average \bar{A}_L appears to converge to some value, it may suddenly deviate from this value and converge to another value as (a). We cannot distinguish this long metastable case (a) from a converged case (b).

(80), we readily have

$$\left| \bar{A} - \frac{1-\alpha}{2} \langle e_2|A|e_2 \rangle \right| \leq \alpha \|A\|, \quad (93)$$

$$\left| \overline{VAV^\dagger} - \frac{1-\alpha}{2} \langle e_2|A|e_2 \rangle \right| \leq 2(\alpha + \sqrt{\alpha(1-\alpha)}) \|A\|, \quad (94)$$

for uniform initial states. This means that both \bar{A} and $\overline{VAV^\dagger}$ converge close to $\frac{1-\alpha}{2} \langle e_2|A|e_2 \rangle$ in the thermodynamic limit with error $\alpha \|A\|$ and $2(\alpha + \sqrt{\alpha(1-\alpha)}) \|A\|$. Since α can be taken arbitrarily small, these relations roughly state that both \bar{A} and $\overline{VAV^\dagger}$ converge around $\frac{1}{2} \langle e_2|A|e_2 \rangle$ with arbitrarily small error.

10.3 What happens if we numerically simulate this system?

We know that for any finite size system \bar{A}_L is computable by exact diagonalization. Therefore, one may wonder what happens if we numerically diagonalize our undecidable system. We here comment on this thought experiment.

Although there are several possible scenarios, we here describe the most intuitive one. We consider the case that TM2 halts after a very long steps. If the system size is insufficient, then the finite control passes the periodic boundary before halting and stops its move. With such small system size, \bar{A}_L takes a value close to zero. On the other hand, if the system size becomes sufficiently large for TM2 to halt, then \bar{A}_L start approaching around $\frac{1}{2} \langle e_2|A|e_2 \rangle$. The problem lies in the fact that we never know what system size is sufficiently large. The undecidability of Turing machines tells that we cannot exclude the possibility that a Turing machine runs for very long steps and suddenly halts. In terms of numerical simulations, any large numerical simulation might be fooled due to insufficient system size, and we cannot distinguish the case with a long metastable state (Fig. 4 (a)) and the case that the system indeed relaxed (Fig. 4 (b)). This clearly explains why exact diagonalization cannot resolve the problem of undecidability.

10.4 Undecidability of thermalization

Our theorems and lemma concern the long-time average after relaxation. We here bridge these results to thermalization, which is announced in our short letter [65]. In the following, we consider the case that a Hamiltonian is input (i.e., HTA case).

Since the observable A is arbitrary as long as $\langle e_1|A|e_1\rangle = 0$ and $\langle e_2|A|e_2\rangle > 0$, we additionally require that A has an eigenstate orthogonal to $|e_0\rangle$ and $|e_1\rangle$ with an eigenvalue a (If needed, we extend the local Hilbert space and set the extended basis as this eigenstate). Let $|\psi_L\rangle = |e_0\rangle \otimes (|e_1\rangle^{\otimes L-1})$ and $E_L := \langle \psi_L|H|\psi_L\rangle$. Then, the equilibrium value of A in the thermodynamic limit is expressed as

$$A_{\text{eq}} = \lim_{L \rightarrow \infty} \frac{1}{L} \text{Tr}[A_L \rho_L^{\text{MC}}(E_L)], \quad (95)$$

where $\rho_L^{\text{MC}}(E_L)$ is a microcanonical ensemble at energy E_L with system size L .

We now tune the eigenvalue a with keeping other eigenvalues of A . Owing to the fact that A_{eq} is a continuous increasing function of a and its range is the whole real number, there exist s^* and s^{**} such that corresponding A_{eq} take respectively zero and $\frac{1}{2} \langle e_2|A|e_2\rangle$. In case with s^* (resp. s^{**}), the initial state $|\psi_L\rangle$ thermalizes with respect to A if and only if TM2 does not halt (resp. halts), which means undecidability of thermalization.

11 Concluding remarks

We have shown that in one-dimensional shift-invariant quantum many-body systems whether the long-time average \bar{A} is in the vicinity of c or not is undecidable. The main idea of our proof is a map from a classical URTM to the Hamiltonian of quantum many-body systems. To make the interaction as nearest-neighbor and shift-invariant, we employ the Feynman-Kitaev type construction of a Hamiltonian.

Our method to implement the halting problem to dynamics of quantum many-body systems will apply to various other problems related to thermalization. However, to encode the halting problem, two cases, the halting case and the non-halting case, should be mapped onto two distinct situations (e.g., thermalizing in one case, and not thermalizing in the other case). Hence, the presence of both two phenomena should be proved in some concrete systems. This fact prevents the extension of our method to the eigenstate thermalization hypothesis because no concrete model is proven to satisfy the eigenstate thermalization hypothesis. In contrast, a recent study proves non-integrability of some concrete models in the sense that the system has no local conserved quantity [54]. Therefore, the decision problem on (non-)integrability for a given Hamiltonian may serve as a stage to extend our method.

We remark that our result does not exclude the possibility that a particular model is proven to thermalize or not to thermalize. Our result excludes the possibility to obtain a general and ultimate criterion to judge the presence or absence of thermalization, but not a model-specific result. In fact, integrable systems are known not to thermalize. We also remark that our model is highly artificial, which is a limitation of our result. We thus have two interesting open problems: One is to find a more *natural* model exhibiting undecidability. The other is to construct a set of more restricted class of Hamiltonians whose fate of thermalization is decidable. Both of problems merit further research.

Acknowledgment

We thank Takahiro Sagawa for stimulating discussion. NS was supported by JSPS Grants-in-Aid for Scientific Research Grant Number JP19K14615.

References

- [1] L. Boltzmann, *Ueber die mechanischen Analogien des zweiten Hauptsatzes der Thermodynamik*. Journal für die reine und angewandte Mathematik **100**, 201 (1887).
- [2] J. von Neumann, *Beweis des Ergodensatzes und des H-Theorems in der neuen Mechanik*. Z. Phys. **57**, 30 (1929) [English version, *Proof of the ergodic theorem and the H-theorem in quantum mechanics*, Eur. Phys. J. H **35**, 201 (2010)] .
- [3] T. Kinoshita, T. Wenger, and D. S. Weiss, *A quantum Newton's cradle*. Nature **440**, 900 (2006).
- [4] S. Trotzky, Y-A. Chen, A. Flesch, I. P. McCulloch, U. Schollwöck, J. Eisert and I. Bloch, *Probing the relaxation towards equilibrium in an isolated strongly correlated one-dimensional Bose gas*. Nat. Phys. **8**, 325 (2012).
- [5] M. Gring, M. Kuhnert, T. Langen, T. Kitagawa, B. Rauer, M. Schreitl, I. Mazets, D. Adu Smith, E. Demler, and J. Schmiedmayer, *Relaxation and Prethermalization in an Isolated Quantum System*, Science **337**, 1318 (2012).
- [6] T. Langen, S. Erne, R. Geiger, B. Rauer, T. Schweigler, M. Kuhnert, W. Rohringer, I. E. Mazets, T. Gasenzer, and J. Schmiedmayer, *Experimental observation of a generalized Gibbs ensemble*, Science **348**, 207 (2015).
- [7] A. M. Kaufman, M. E. Tai, A. Lukin, M. Rispoli, R. Schittko, P. M. Preiss, and M. Greiner, *Quantum thermalization through entanglement in an isolated many-body system*. Science **353**, 794 (2016).
- [8] H. Bernien, S. Schwartz, A. Keesling, H.y Levine, A. Omran, H. Pichler, S. Choi, A. S. Zibrov, M. Endres, M. Greiner, V. Vuletic, and M. D. Lukin, *Probing many-body dynamics on a 51-atom quantum simulator*. Nature **551**, 579 (2017).
- [9] C. J. Turner, A. A. Michailidis, D. A. Abanin, M. Serbyn, and Z. Papić, *Weak ergodicity breaking from quantum many-body scars*. Nature Physics **14**, 745 (2018).
- [10] C.-J. Lin and O. I. Motrunich, *Exact Quantum Many-Body Scar States in the Rydberg-Blockaded Atom Chain*. Phys. Rev. Lett. **122**, 173401 (2019).
- [11] W. W. Ho, S. Choi, H. Pichler, and M. D. Lukin, *Periodic Orbits, Entanglement, and Quantum Many-Body Scars in Constrained Models: Matrix Product State Approach*. Phys. Rev. Lett. **122**, 040603 (2019).
- [12] N. Shiraishi, *Connection between quantum-many-body scars and the AKLT model from the viewpoint of embedded Hamiltonians*. J. Stat. Mech. 083103 (2019).
- [13] M. Serbyn, D. A. Abanin, and Z. Papić, *Quantum Many-Body Scars and Weak Breaking of Ergodicity*. arXiv:2011.09486.
- [14] S. Lloyd, *Black Holes, Demons, and the Loss of Coherence*, Ph.D. Thesis, Rockefeller University, (1988).
- [15] S. Popescu, A. J. Short, and A. Winter, *A. Entanglement and the foundations of statistical mechanics*. Nat. Phys. **2**, 754 (2006).

- [16] S. Goldstein, J. L. Lebowitz, R. Tumulka, and N. Zanghi, *Canonical typicality*. Phys. Rev. Lett. **96**, 050403 (2006).
- [17] A. Sugita, *On the foundation of quantum statistical mechanics*. (in Japanese) RIMS (Res. Inst. Math. Sc., Kyoto) Kokyuroku **1507**, 147 (2006).
- [18] P. Reimann, *Typicality for generalized microcanonical ensembles*. Phys. Rev. Lett. **99**, 160404 (2007).
- [19] H. Tasaki, *Typicality of Thermal Equilibrium and Thermalization in Isolated Macroscopic Quantum Systems*. J. Stat. Phys. **163**, 937 (2016).
- [20] C. Bartsch and J. Gemmer, *Dynamical Typicality of Quantum Expectation Values*. Phys. Rev. Lett. **102**, 110403 (2009).
- [21] S. Goldstein¹, T. Hara and H. Tasaki, *Extremely quick thermalization in a macroscopic quantum system for a typical nonequilibrium subspace*. New J. Phys. **17** 045002 (2015).
- [22] P. Reimann, *Typical fast thermalization processes in closed many-body systems*. Nat. Comm. **7**, 10821 (2016).
- [23] L. Dabelow and P. Reimann. *Relaxation Theory for Perturbed Many-Body Quantum Systems versus Numerics and Experiment*. Phys. Rev. Lett. **124**, 120602 (2020).
- [24] J. M. Deutsch, *Quantum statistical mechanics in a closed system*. Phys. Rev. A **43**, 2046 (1991).
- [25] M. Srednicki, *Chaos and quantum thermalization*. Phys. Rev. E **50**, 888 (1994).
- [26] M. Horoi, V. Zelevinsky, and B. A. Brown, *Chaos vs Thermalization in the Nuclear Shell Model*. Phys. Rev. Lett. **74**, 5194 (1995).
- [27] H. Tasaki, *From Quantum Dynamics to the Canonical Distribution: General Picture and a Rigorous Example*. Phys. Rev. Lett. **80**, 1373 (1998).
- [28] M. Rigol, V. Dunjko, M. Olshanii, *Thermalization and its mechanism for generic isolated quantum systems*. Nature **452**, 854 (2008).
- [29] G. Biroli, C. Kollath, and A. M. Läuchli, *Effect of Rare Fluctuations on the Thermalization of Isolated Quantum Systems*. Phys. Rev. Lett. **105**, 250401 (2010).
- [30] N. Shiraishi and T. Mori, *Systematic Construction of Counterexamples to Eigenstate Thermalization Hypothesis*. Phys. Rev. Lett. **119**, 030601 (2017).
- [31] T. Mori and N. Shiraishi, *Thermalization without eigenstate thermalization hypothesis after a quantum quench*. Phys. Rev. E **96**, 022153 (2017).
- [32] S. Moudgalya, S. Rachel, B. A. Bernevig, and N. Regnault, *Exact Excited States of Non-Integrable Models*. Phys. Rev. B **98**, 235155 (2018).
- [33] S. Moudgalya, N. Regnault, and B. A. Bernevig, *Entanglement of exact excited states of Affleck-Kennedy-Lieb-Tasaki models: Exact results, many-body scars, and violation of the strong eigenstate thermalization hypothesis*. Phys. Rev. B **98**, 235156 (2018).

- [34] N. Shiraishi, *Analytic model of thermalization: Quantum emulation of classical cellular automata*. Phys. Rev. E **97**, 062144 (2018).
- [35] T. Mori, *Weak eigenstate thermalization with large deviation bound*. arXiv:1609.09776 (2016).
- [36] P. Reimann, *Foundation of Statistical Mechanics under Experimentally Realistic Conditions*. Phys. Rev. Lett. **101**, 190403 (2008).
- [37] N. Linden, S. Popescu, A. J. Short, and A. Winter, *Quantum mechanical evolution towards thermal equilibrium*. Phys. Rev. E **79**, 061103 (2009).
- [38] A. J. Short and T. C. Farrelly, *Quantum equilibration in finite time*. New J. Phys. **14**, 013063 (2012).
- [39] T. Farrelly, F.G.S.L. Brandao, M. Cramer, *Thermalization and Return to Equilibrium on Finite Quantum Lattice Systems*. Phys. Rev. Lett. **118**, 140601 (2017).
- [40] D. M. Basko, I. L. Aleiner, and B. L. Altshuler, *Metal-insulator transition in a weakly interacting many-electron system with localized single-particle states*. Ann. Phys. **321**, 1126 (2006).
- [41] A. Pal and D. A. Huse, *Many-body localization phase transition*. Phys. Rev. B **82**, 174411 (2010).
- [42] E. Hamza, R. Sims, and G. Stolz, *Dynamical Localization in Disordered Quantum Spin Systems*. Commun. Math. Phys. **315**, 215 (2012).
- [43] M. Serbyn, Z. Papić, and D. A. Abanin, *Local Conservation Laws and the Structure of the Many-Body Localized States*. Phys. Rev. Lett. **111**, 127201 (2013).
- [44] M. Friesdorf, A. H. Werner, W. Brown, V. B. Scholz, and J. Eisert, *Many-Body Localization Implies that Eigenvectors are Matrix-Product States*. Phys. Rev. Lett. **114**, 170505 (2015).
- [45] R. Nandkishore and D. A. Huse, *Many body localization and thermalization in quantum statistical mechanics*. Ann. Rev. Cond. Matt. Phys. **6** 15 (2015).
- [46] J. Z. Imbrie, *On Many-Body Localization for Quantum Spin Chains*, J. Stat. Phys. **163**, 998 (2016).
- [47] M. A. Cazalilla, *Effect of Suddenly Turning on Interactions in the Luttinger Model*. Phys. Rev. Lett. **97**, 156403 (2006).
- [48] M. Rigol, V. Dunjko, V. Yurovsky, and M. Olshanii, *Relaxation in a Completely Integrable Many-Body Quantum System: An Ab Initio Study of the Dynamics of the Highly Excited States of 1D Lattice Hard-Core Bosons*. Phys. Rev. Lett. **98**, 050405 (2007).
- [49] E. Ilievski, J. De Nardis, B. Wouters, J.-S. Caux, F. H. L. Essler, and T. Prosen, *Complete Generalized Gibbs Ensembles in an Interacting Theory*. Phys. Rev. Lett. **115**, 157201 (2015).
- [50] F. Essler and M. Fagotti, *Quench dynamics and relaxation in isolated integrable quantum spin chains*. J. Stat. Mech. 064002 (2016).

- [51] C. Gogolin, M. P. Müller, and J. Eisert, *Absence of Thermalization in Nonintegrable Systems*. Phys. Rev. Lett. **106**, 040401 (2011).
- [52] H. Kim, M. C. Bañuls, J. I. Cirac, M. B. Hastings, and D. A. Huse, *Slowest local operators in quantum spin chains*, Phys. Rev. E **92**, 012128 (2015).
- [53] L. P. García-Pintos, N. Linden, A. S. L. Malabarba, A. J. Short, and A. Winter, *Equilibration Time Scales of Physically Relevant Observables*. Phys. Rev. X **7**, 031027 (2017).
- [54] N. Shiraishi, *Proof of the absence of local conserved quantities in the XYZ chain with a magnetic field*. Europhys. Lett. **128**, 17002 (2019) .
- [55] C. Gogolin and J. Eisert, *Equilibration, thermalisation, and the emergence of statistical mechanics in closed quantum systems*. Rep. Prog. Phys. **79**, 056001 (2016).
- [56] C. Moore, *Unpredictability and undecidability in dynamical systems*. Phys. Rev. Lett. **64**, 2354 (1990).
- [57] J. Eisert, M. P. Müller, and C. Gogolin, *Quantum measurement occurrence is undecidable*. Phys. Rev. Lett. **108**, 260501 (2012).
- [58] T. S. Cubitt, D. Perez-Garcia and M. M. Wolf, *Undecidability of the spectral gap*. Nature **528**, 207 (2015).
- [59] A. M. Turing, *On computable numbers, with an application to the Entscheidungsproblem*. Proc. London Math. Soc. **42**, 230 (1937).
- [60] C. Moore and S. Mertens, *Nature of computation*. Oxford university press (2011).
- [61] R. Feynman, *Quantum mechanical computers*. Optics News **11**, 11 (1985).
- [62] A. Yu. Kitaev, A.H. Shen, and M.N. Vyalyi. *Classical and Quantum Computation*. Vol. 47 of Graduate Studies in Mathematics. American Mathematical Society, (2002).
- [63] P. Bocchieri and A. Loinger, *Quantum Recurrence Theorem*. Phys. Rev. **107**, 337 (1957).
- [64] K. Morita, *Theory of Reversible Computing*. Springer (2017).
- [65] N. Shiraishi and K. Matsumoto, appear on arXiv on the same date as this manuscript.